

# Four Element EC Slot MIMO Antenna for WLAN, Wi-Fi, and 5G Applications

Sachin S. Khade<sup>1,\*</sup>, Dinesh B. Bhoyar<sup>1</sup>, Ketki Kotpalliwar<sup>1</sup>,  
Chitra V. Bawankar<sup>2</sup>, and Manish S. Kimmatkar<sup>3</sup>

<sup>1</sup>Yeshwantrao Chavan College of Engg, Nagpur, India

<sup>2</sup>GHRIET, Nagpur, India

<sup>3</sup>SRPCE, Nagpur, India

**ABSTRACT:** The architecture of antenna is with four elements design for 5G, Wi-Max, Wi-Fi, and WLAN applications. The operating range of the antenna covers the frequency band from 4.72 GHz to 5.24 GHz. The antenna has dimensions of  $46 \times 46 \times 1.6 \text{ mm}^3$  with four elements. The antenna is designed with a planer monopole having two matching stubs connected at the lower end. All the elements of antenna contain E and C shaped slots and two identical stubs providing capacitive effect. The gain of the designed antennas ranges from 2.23 dB to 2.73 dB for desired bands. The designed antenna shows suitability for 4.9 GHz WLAN band, 5 GHz and 5.15 GHz Wi-Fi and Wi-Max bands. Also it covers part of the n79 5G band.

## 1. INTRODUCTION

Upcoming technology of wireless networking requires a compact [1] antenna due to rapid rise of its usability. Antenna plays a very critical role in wireless systems. Multiple-input multiple-output (MIMO) antenna has outstanding feature of the 5G compatibility [2, 14]. MIMO antenna shows the ability to improve communication spectral efficiency [15] over a broad range of application. MIMO antenna technology for wireless communication [13] makes use of multiple antennas [4, 5] at both the transmitting and receiving ends. It assists minimizing errors, optimized data speed and improves the capacity of wireless transmissions by allowing data to transmit at the same time over multiple signal paths. It creates multiple types of same signals. MIMO gives more opportunities for the transmitted data to reach receiving end without being affected by fading [3], which helps to enhance the signal-to-noise ratio and reduce bit error rate. MIMO shows less congestion with connection stability [8]. This is achieved by aggregating signals from each of its antennas to clean up a noisy signal [6], resulting in faster signal processing and faster data transmission. The advantage shown by MIMO antenna is high data rate [11] by utilizing different combinations of Tx and Rx, time diversity, frequency diversity, and multipath phenomenon, which helps to reduce signal distortion [7]. Defected ground structure (DGS) is a compact geometrically small slot [1, 10, 16] embedded on the ground plane of printed microstrip board [9]. It is a purposefully created defect and is typically an etched out pattern on ground plane. DGS is used for the enhancement of radiation pattern and bandwidth of antenna. MIMO allows the utilization of a large number of devices connected [12]. The effective electrical length of antenna is increased after the integration of

a dumbbell DGS which shifts the resonance frequency [17]. MIMO antenna gives us the solution to deal with challenges and also increases the volume by the transmission of signals to multiple antennas [14]. Partially reflective surface is incorporated to improve the antenna gain by controlling its phase characteristics [18].

## 2. ANTENNA DESIGN

### 2.1. Material and Configuration

The antenna is designed by integrating four square shaped patch elements in single unit. It is broadly used because of its unique advantages like light weight, cost effective, conformal, and low profile. Compactness and aesthetics are preferred for antennas. FR-4 substrate is used to make it cost effective with some structural simplicity. The patch element and ground are made up of piece of metal (here, copper). The substrate is sandwiched between the ground and radiating elements. The FR4 substrate is a substrate with good strength and low dielectric loss, and supports the antenna mechanically as well as electrically.

The antenna consists of four rectangular elements with stubs and E and C shaped slots etched on it. It has a square shaped block at the center. The placing of all the four elements is symmetrical to the center of the antenna structure. The stubs used in each element provide an induced capacitive effect. The slots etched on each element are useful for size reduction of the antenna.

The back side of the antenna comprises a square shaped ground component with a square slot at the center. Considering the aesthetic aspects, the design of MIMO is kept symmetrical. Here we have used probe feeding method for all the elements.

\* Corresponding author: Sachin S. Khade (sac\_mob@rediffmail.com).

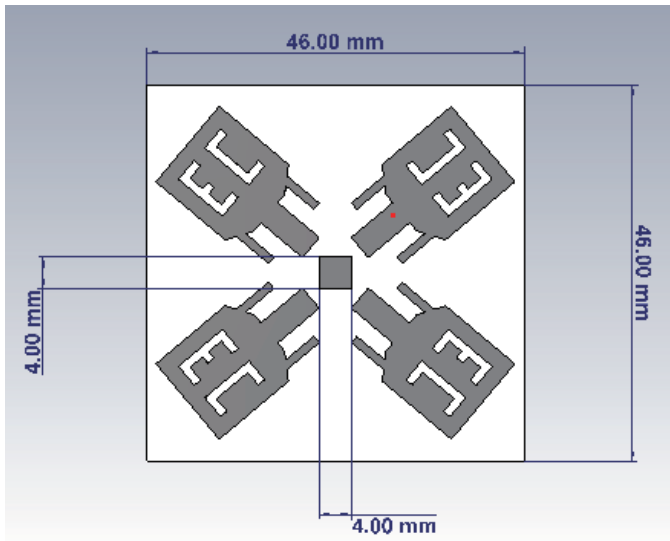


FIGURE 1. Front view.

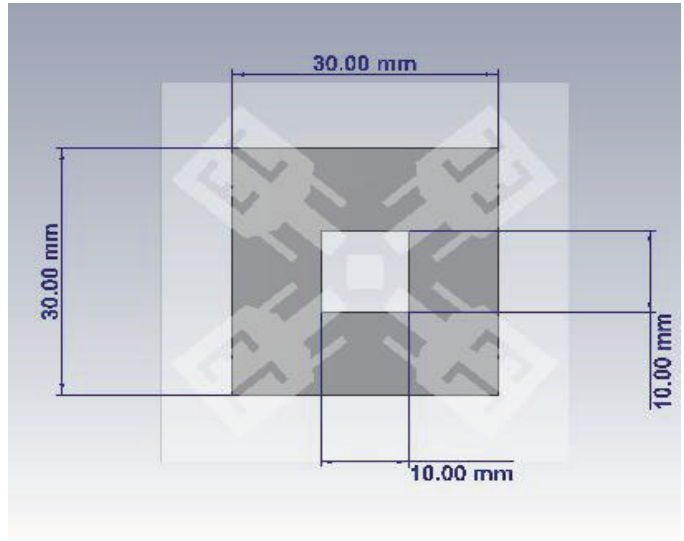


FIGURE 2. Back view.

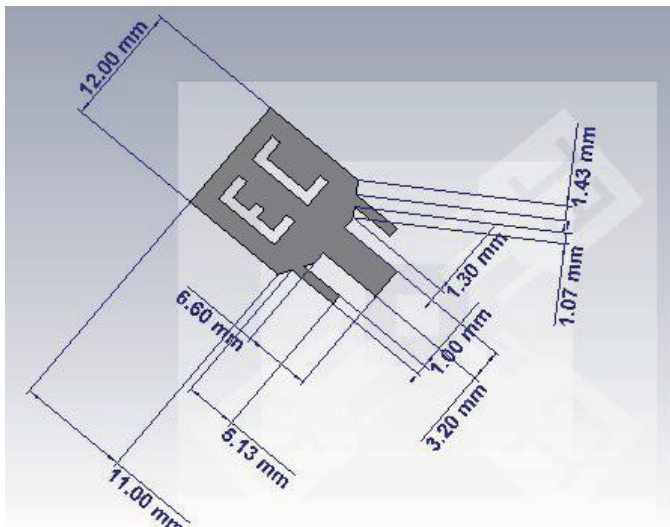


FIGURE 3. Dimension of each element.

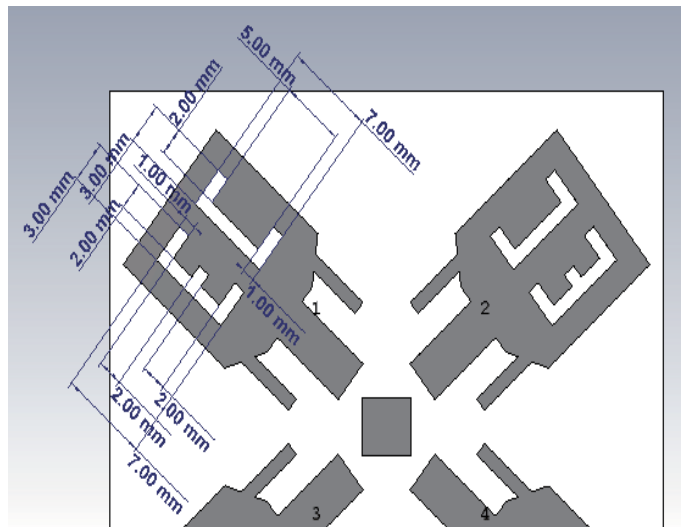


FIGURE 4. Dimensions of E and C slot.

## 2.2. Geometry of The Proposed Antenna

The detailed antenna geometry shows four rectangular elements with E and C slots and two identical stubs inclined at  $45^\circ$  with the main axis, presented in Figure 1 (front view) and 2 (back View). The dimensions of each used element are depicted in Figures 3 and 4.

## 2.3. Evolution of Design

The flow diagrams from Figures 5 to 8 express the gradual process of evolution of a four element antenna. After introducing all the four elements of the antenna over the substrate, we placed it in a symmetrical fashion. All the elements show symmetry with the center and are inclined at  $45^\circ$  with the nearest axis.

Initially the size of the substrate is optimized. Then, the patch is copied using the mirror function. In this fashion, we attained

our final design for MIMO with four elements and ports, respectively. Each patch contains two identical stubs, E and C shaped slots. The stubs help in matching the impedance. Partial ground is introduced initially at the back side. Then, the slots are inserted which improves surface current and increases gain as well as bandwidth.

$$W_p = \frac{c}{4f_o \sqrt{\frac{\epsilon_r + 1}{2}}} \quad (1)$$

$$L_{patch} = \frac{c}{4f_o \epsilon_{eff}} \quad (2)$$

$$\epsilon_{eff} = \frac{\epsilon_r + 1}{2} + \frac{\epsilon_r - 1}{2} \frac{1}{\sqrt{1 + 12 \frac{h}{w_p}}} \quad (3)$$

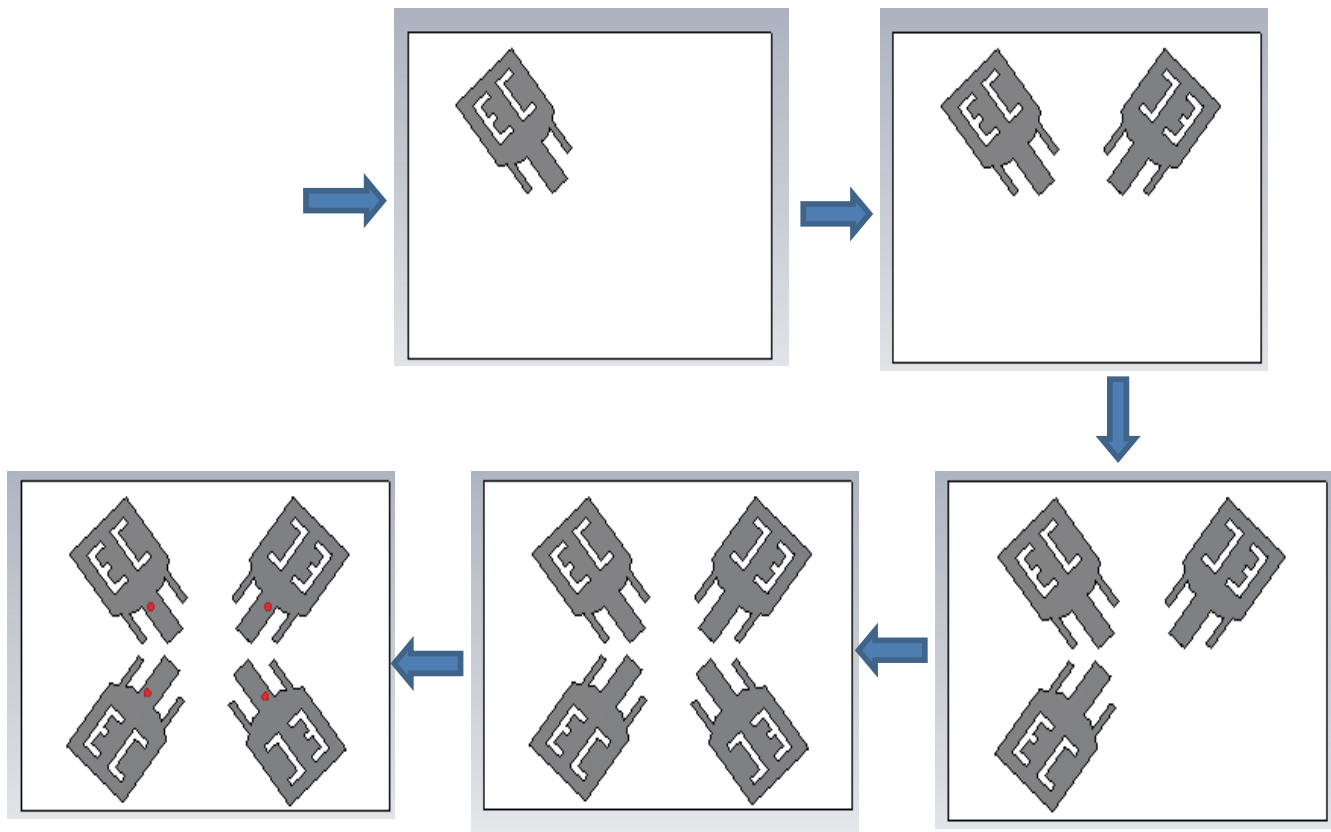


FIGURE 5. Design process.

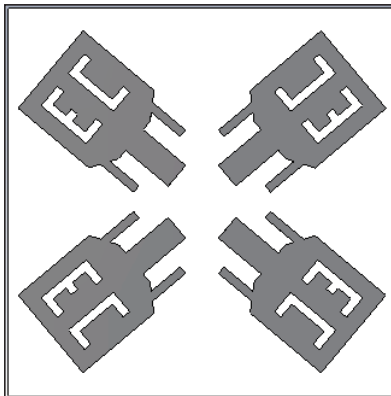


FIGURE 6. Final design (symmetrical).

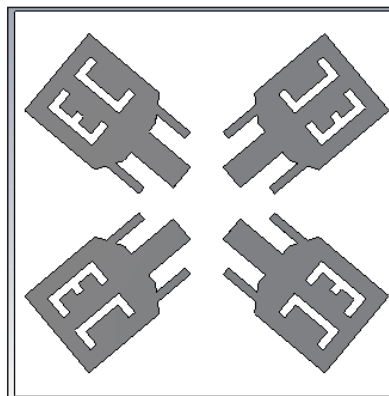


FIGURE 7. Front view of MIMO antenna.

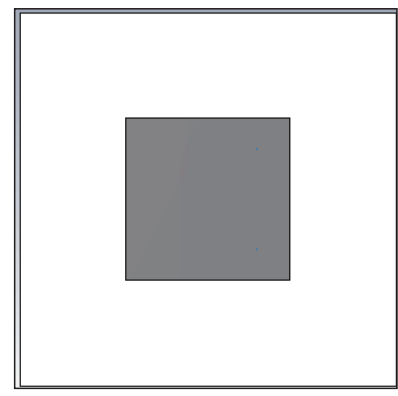


FIGURE 8. Back view of MIMO antenna.

### 3. DESIGN AND RESULTS

#### 3.1. Design with Partial Ground Plane

Initially, we have used a four element MIMO antenna with a partial square shaped ground ( $20 \times 20$  mm) and simulated the results.

Simulation results of our design show only one band from 6.08 GHz to 6.42 GHz, as depicted in Figure 9. For the desired results we have to shift the band towards desired band of frequencies. For that we have to introduce some changes to the design. Changes have been made in design such as shifting the

ports and changing the dimensions of ground, as mentioned in Figures 10 and 11.

#### 3.2. Design with a Center Block

Here, we need introduce a square block element at the center of the design and also shift the ports towards the center. Then, a square parasitic element of  $4 \times 4$  mm<sup>2</sup> is added at the center. Also, the size of the ground is modified to  $10 \times 10$  mm<sup>2</sup>.

Figure 12 shows the simulation results after introducing the changes. Here, we get a single band which is from 6.07 GHz to 6.41 GHz. We still require certain changes to acquire the

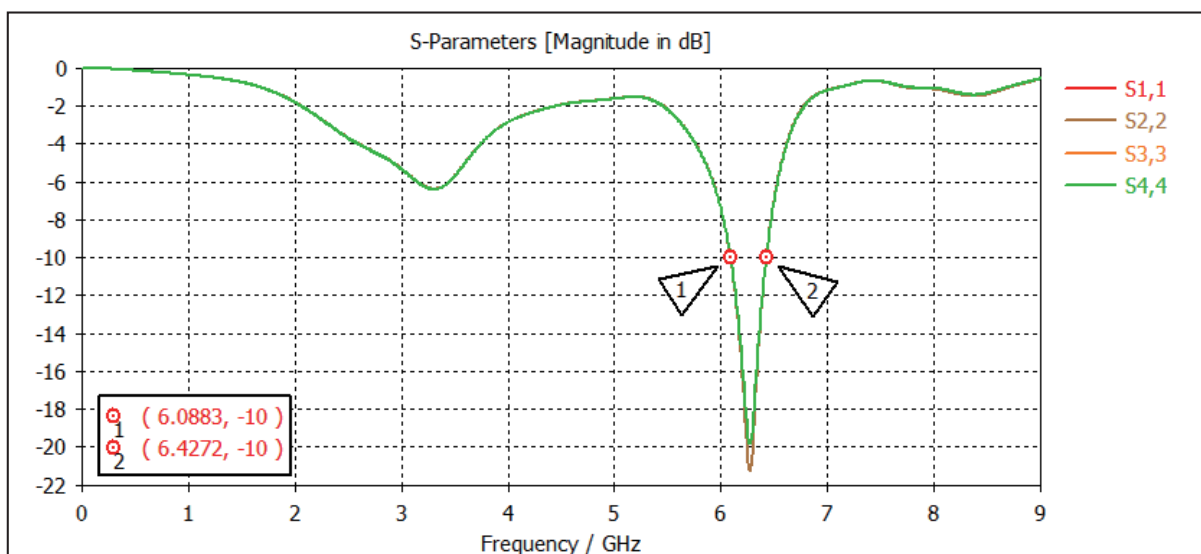


FIGURE 9. Simulation results.

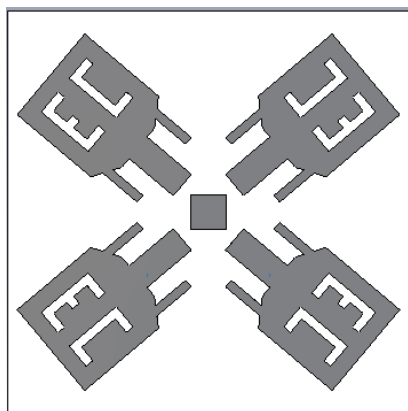


FIGURE 10. Front view of MIMO antenna with a central block.

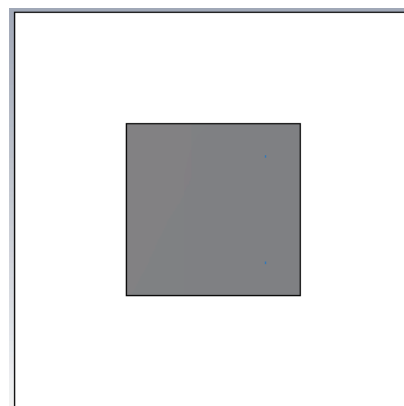


FIGURE 11. Back view of MIMO antenna with a central block.

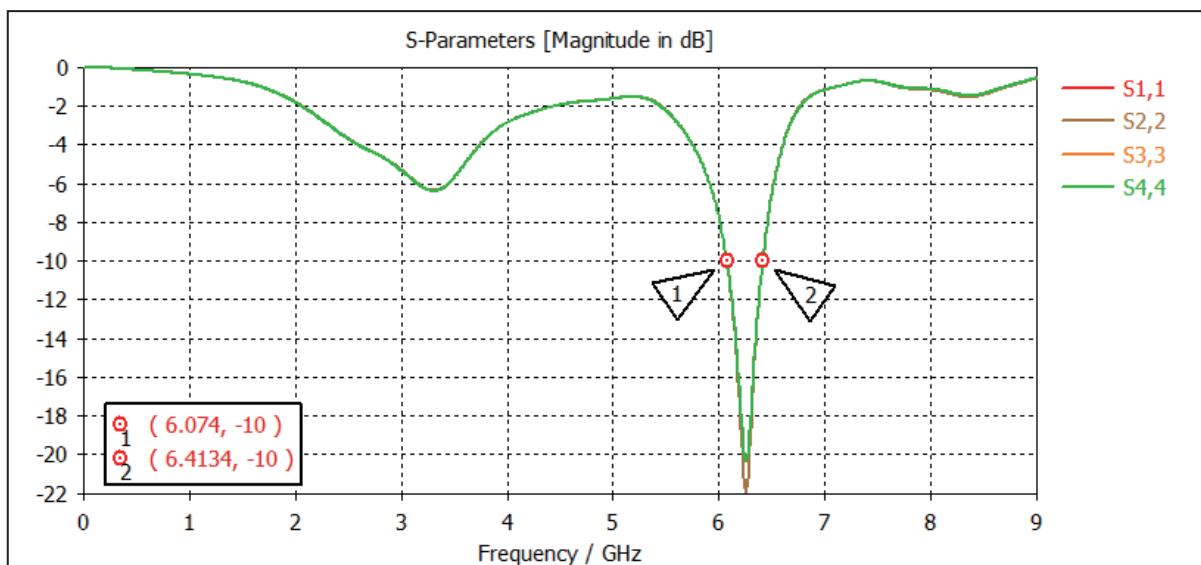


FIGURE 12. Simulation results with a central block.

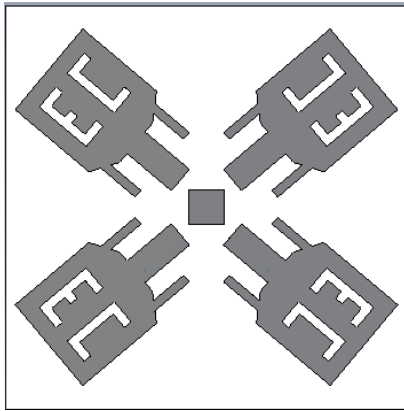


FIGURE 13. Front view of antenna with square shaped DGS.

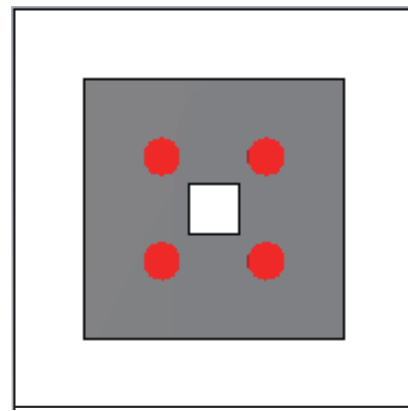


FIGURE 14. Back view of antenna with square shaped DGS.

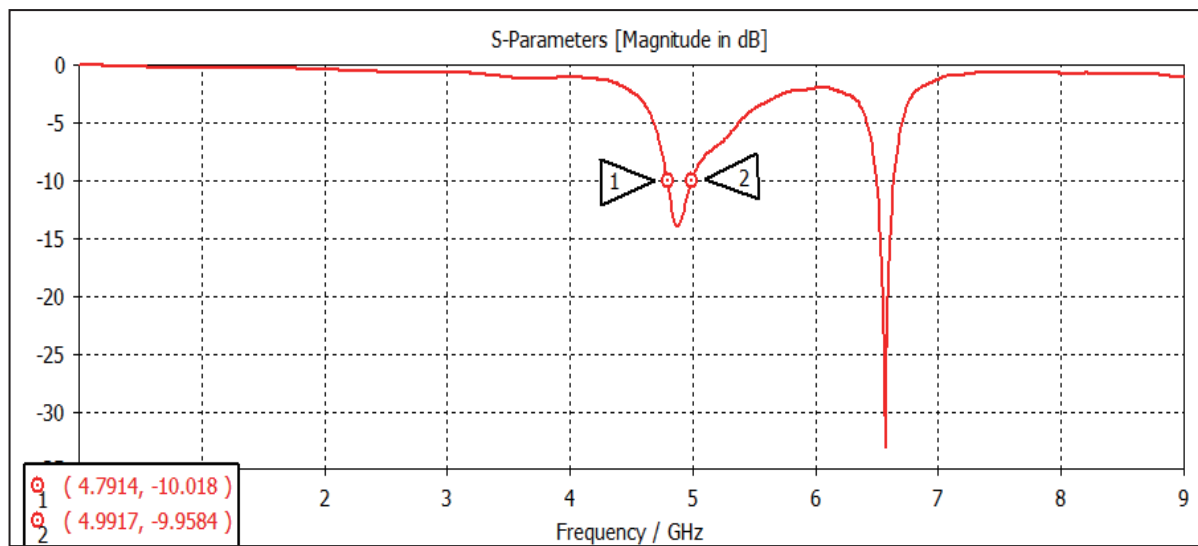


FIGURE 15. Simulation results of antenna with square shaped DGS.

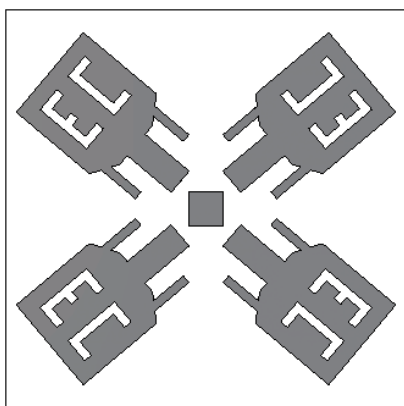


FIGURE 16. Front view of MIMO.

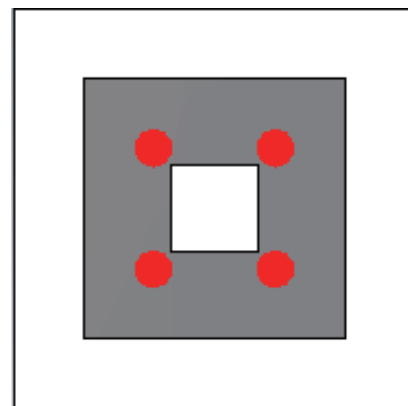
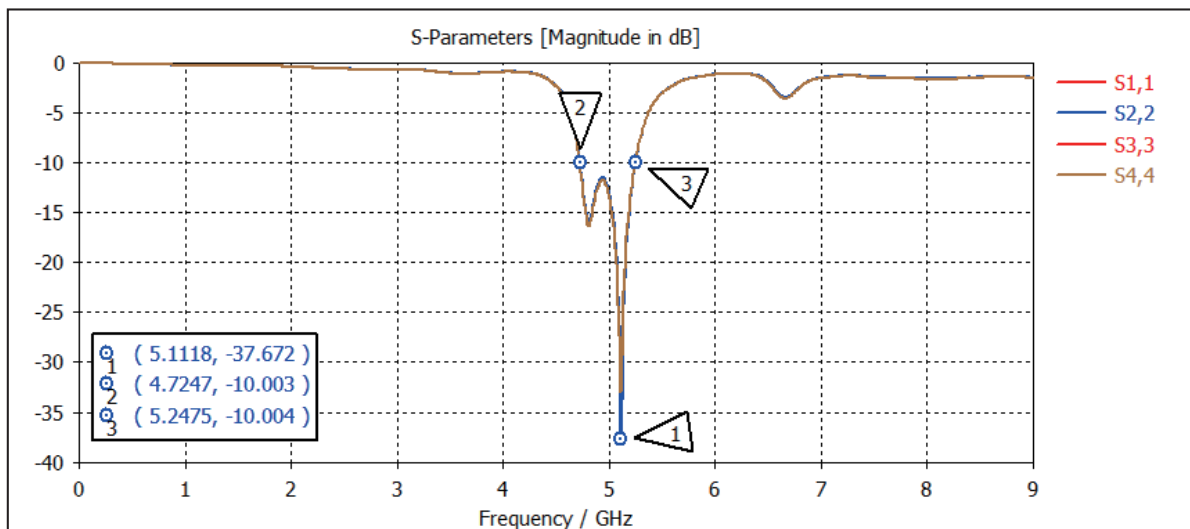


FIGURE 17. Back view of MIMO.



**FIGURE 18.** Simulated reflection coefficient results of MIMO antenna with DGS.

desired frequency bands. To further shift the band toward its left, we have to introduce defect in the ground plane.

### 3.3. Design with DGS

Defected ground structure (DGS) is a compact geometrically slot embedded on ground plane of printed Microstrip panel. It is a purposefully created defect. It is typically a part which is removed from ground plane. DGS is used for shifting the operating band to targeted range. Also, it is used for the enhancement of gain and bandwidth. Here, we introduce a square shape defect of  $5 \times 5 \text{ mm}^2$  at the center over a  $30 \times 30 \text{ mm}^2$  square ground plane.

After simulation of the design shown in Figures 13 and 14, the results of reflection coefficients are depicted in Figure 15. With the changes to the ground, our simulation result shows a band of frequencies from 4.7 to 4.9 GHz, which covers our desired range of frequencies. For further improvement of the results in terms of gain and bandwidth, we have to introduce further changes in the design.

### 3.4. Design of MIMO with four Elements and DGS

Here, the final design of our Quad MIMO antenna for 5G application with a DGS is presented in Figures 16 and 17. The square shaped defect is optimized to  $10 \times 10 \text{ mm}^2$  through parametric analysis. The ports are placed symmetrically with a separation of 14 mm.

Figures 18 and 19 demonstrate the simulation results for the designed antenna. Here, we observe the design to operate over a band of frequencies from 4.72 to 5.24 GHz with resonance at 5.11 GHz. This band covers our desired frequencies which are 4.9 GHz (WLAN), 5 GHz and 5.15 GHz (Wi-Max and Wi-Fi). It also covers n79 5G band frequencies. The maximum depth, i.e., resonance, is obtained at frequency 5.11 GHz.

The above succession of figures from Figure 20 to Figure 22 shows the combined gain in 3D and 2D with respect to all ports.

The natural electromagnetic radiation behavior is depicted by the far field. Radiation pattern is an antenna concept which describes directional frequency dependence of radio waves emitted by an antenna. The gain of antenna with respect to application frequencies are 2.23 dB at 4.9 GHz, 2.73 dB at 5 GHz, and 2.33 dB at 5.15 GHz. The proposed design of the antenna shows good spectral efficiency at desired frequency range. Figure 23 represents the series of surface current with respect to port 2 at the respective frequencies. The surface current depicts the flow of electric current actually induced by an electromagnetic field applied. Simply, it provides us with a perspective of how the current flows. The electric field pushed the charges around. The signals are distinctively added at 4.9 GHz frequency. The radiation pattern shows one major lobe and a back lobe. The antenna radiates omnidirectionally with vertical polarization and donut like radiation pattern. At 5 GHz frequency, there is constructive addition of signal with a total gain of 2.73 dB. The radiation pattern shows one major lobe and a back lobe. The antenna radiates omnidirectionally with horizontal polarization and butterfly like radiation pattern. Similarly, the antenna shows constructive addition with a total gain of 2.33 dB. The radiation pattern shows one major lobe and a back lobe. The antenna radiates omnidirectionally with horizontal polarization and symmetrical radiation pattern with respect constant phi. The plot of cross polarization depicted in Fig. 20(B) indicates a good degree of diversity which has been achieved by the proposed antenna.

Correlation characteristics and port isolation are the required parameters to assess the working performance of the MIMO antenna. The diversity performance of the projected MIMO antenna including diversity gain (DG) and environmental correlation coefficient (ECC) has been studied to demonstrate the durability of the proposed antenna design. These are the important aspects in concern with measure of antenna performance. Here, correlation coefficient of antenna between consecutive and apposite elements is found well below 0.05 at all the targeted frequencies, which is indicated in Figure 24. The mea-

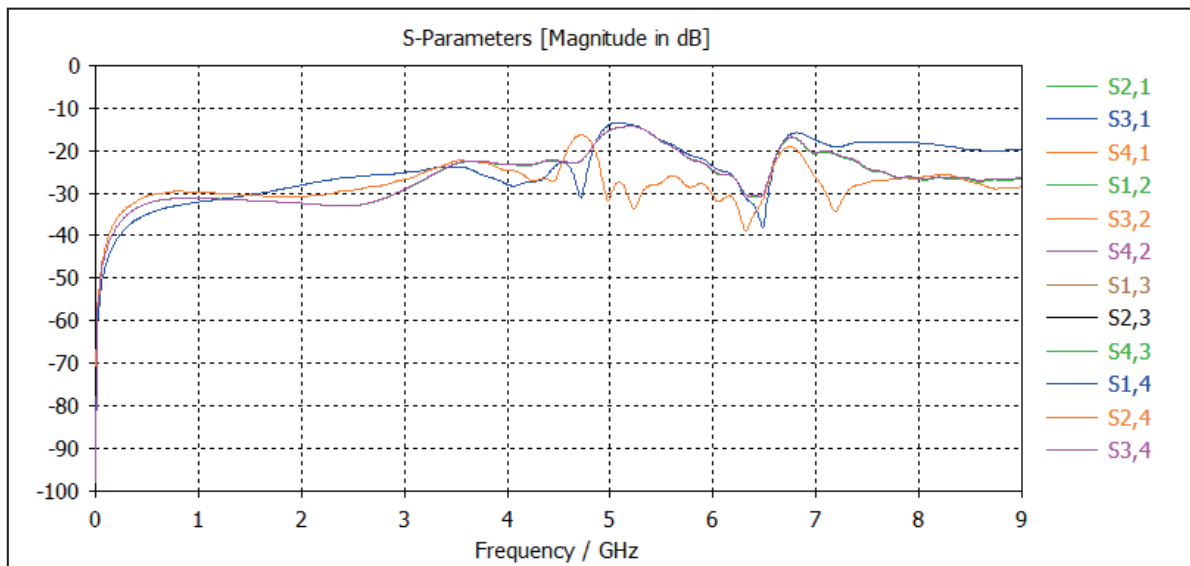


FIGURE 19. Simulated transmission coefficient results of MIMO antenna with DGS.

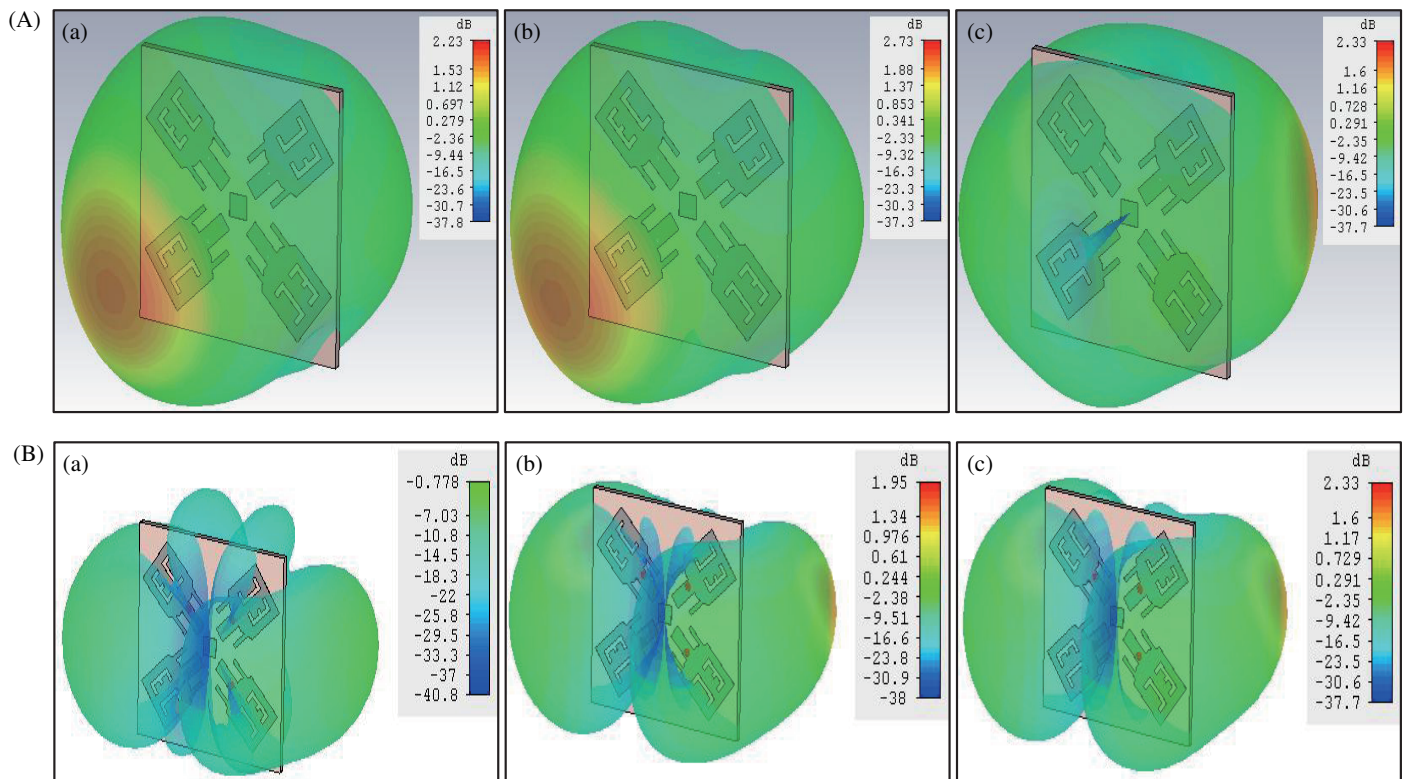


FIGURE 20. (A) Gain in 3D form at (a) 4.9 GHz (b) 5 GHz and (c) 5.15 GHz. (B) Cross Polarization at (a) 4.9 GHz (b) 5 GHz and (c) 5.15 GHz.

sured ECC can be calculated using the formula given below:

$$ECC = \frac{|S_{11}^* S_{12} + S_{21}^* S_{22}|}{(1 - |S_{11}|^2 - |S_{21}|^2)(1 - |S_{22}|^2 - |S_{12}|^2)} \quad (4)$$

The calculated value of ECC at resonance is found 0.0031. ECC shows the way how the elements of the system correlate with each other with respect to their particular individual properties. It also shows how good the channel isolation in wireless

communication network is. It can be determined from the  $S$ -parameter and far field radiation, and it should be less than 0.05 at resonant frequency.

DG is also a MIMO antenna system performance metric. It demonstrates how the diversity scheme affects the power radiated. It shows that all the four elements have less correlation with each other, and their gains are diversified, i.e., they have their main lobes in different directions. Here, the diversity of

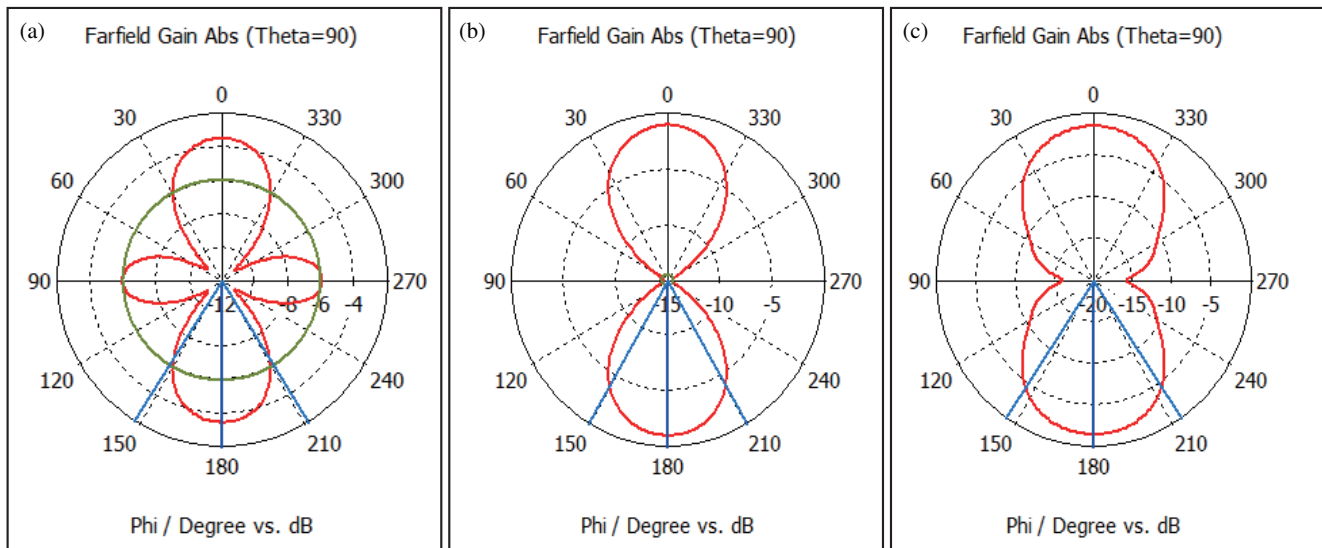


**FIGURE 21.** 2D Gain with constant theta at frequencies, (a) 4.9 GHz, (b) 5 GHz, (c) 5.15 GHz.

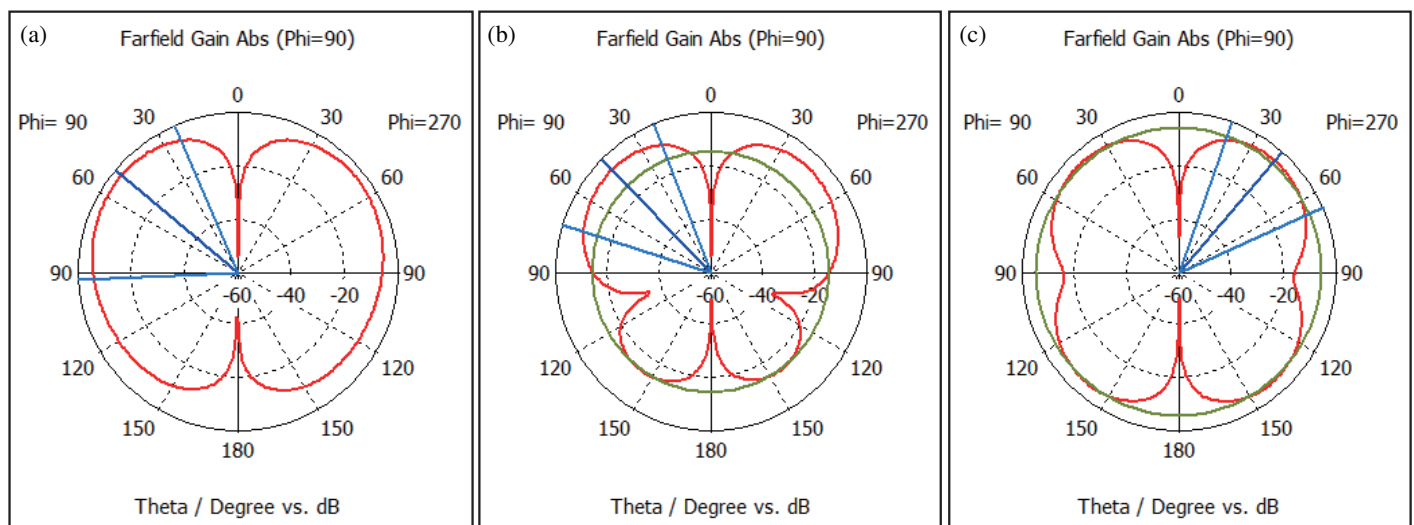


**FIGURE 22.** 2D Gain with constant Phi at frequencies, (a) 4.9 GHz, (b) 5 GHz, (c) 5.15 GHz.

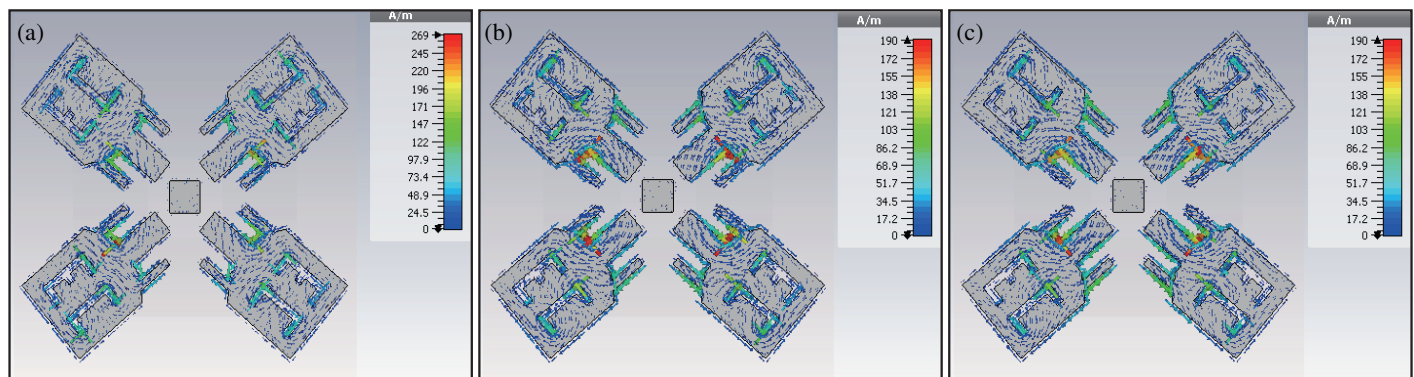


**FIGURE 23.** Surface currents of antenna at (a) 4.9 GHz, (b) 5 GHz, (c) 5.15 GHz.

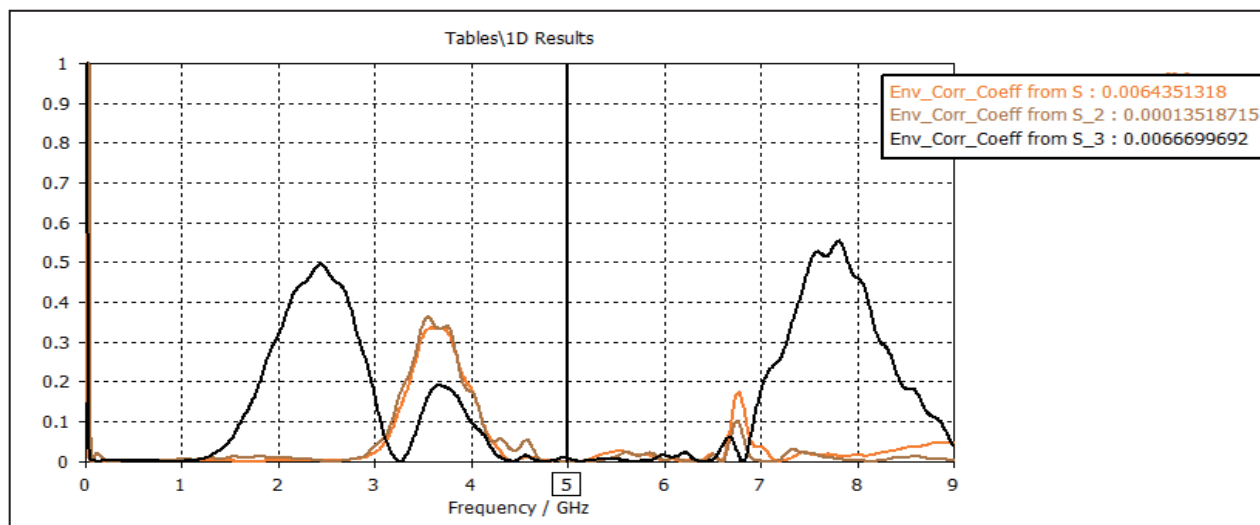


FIGURE 24. ECC for the MIMO antenna.

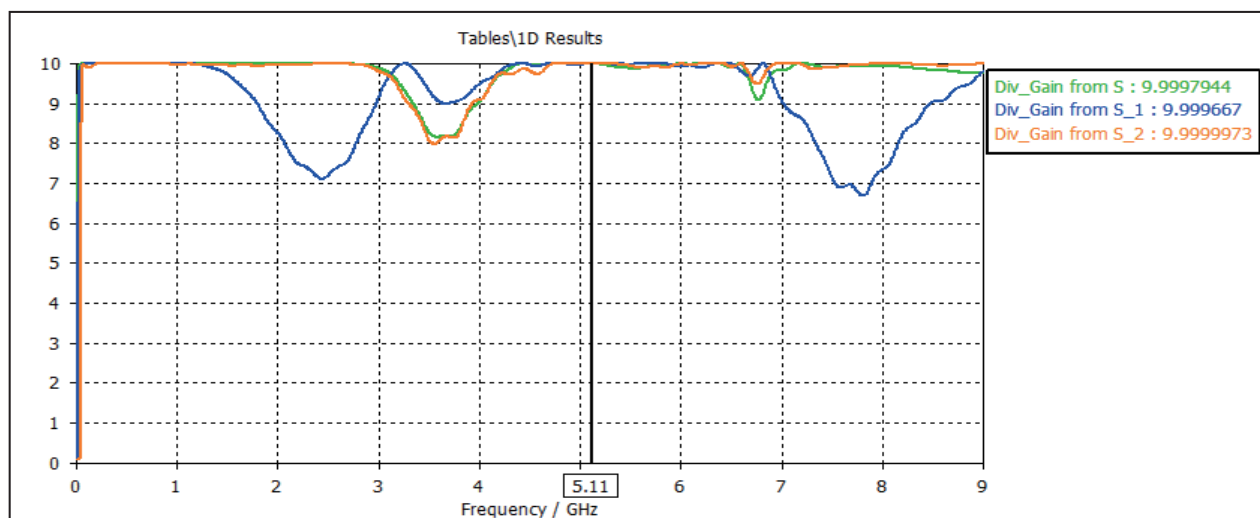


FIGURE 25. Diversity gain for MIMO antenna.

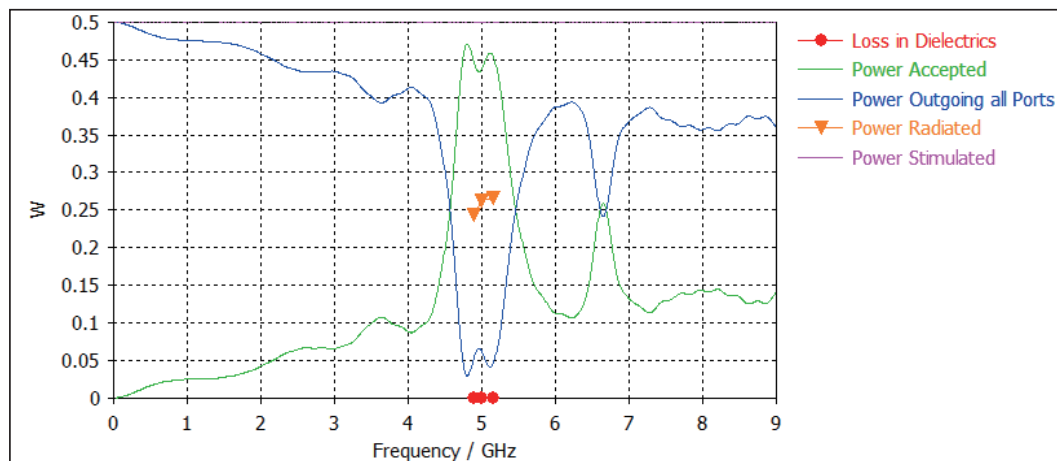
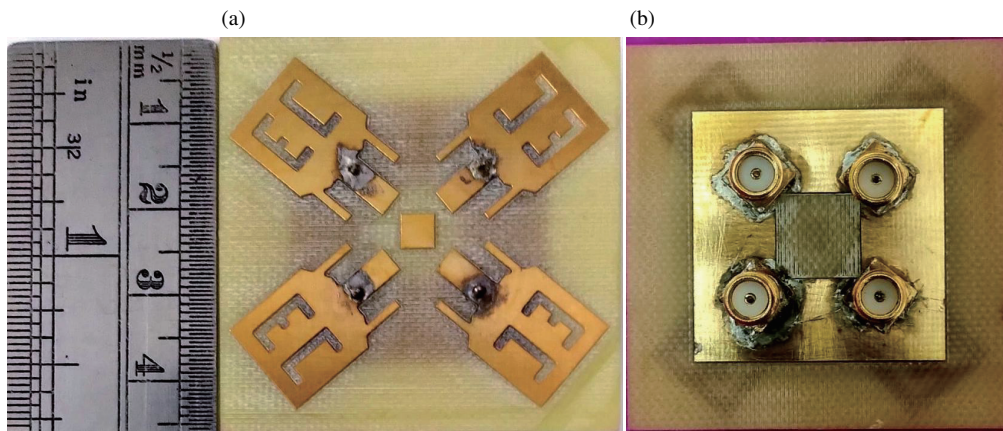
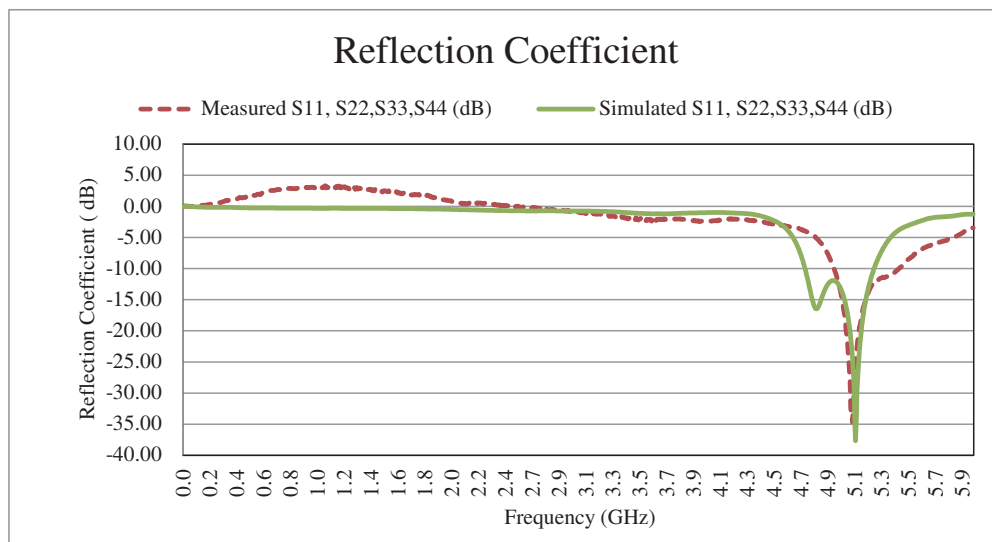


FIGURE 26. Power pattern of MIMO antenna.



**FIGURE 27.** (a) Front view and (b) back view of the fabricated antenna.



**FIGURE 28.** Comparison of reflection coefficients.

antenna between consecutive and apposite elements is found around 10 at all the targeted frequencies, as per the simulated results shown in Figure 25.

Power pattern shows the measured radiated energy of the antenna system. From Figure 26, we found that the antenna accepts the power in the operating frequency range and then radiates part of that. The maximum efficiency of antenna is found around 60%.

#### 4. PROTOTYPE OF THE MIMO ANTENNA

The proposed antenna design is fabricated using etching method, and the ports are connected to it. The structure of fabricated antenna is presented in Figure 27. As stated above, the overall size of the antenna is  $46 \times 46 \text{ mm}^2$ , and it is indicated in the figure by comparing it with measuring scale.

The comparative results of proposed antenna are presented in Figures 28 and 29. There is a slight difference between the

simulated and measured results of the projected MIMO antenna system. This may be because of the soldering, physical material, and the present environmental surrounding and its impact. The solid line specifies the simulated results while the dotted line specifies the measured results. The antenna is well appropriate for the n79-5G band, 4.9 GHz (WLAN), 5 and 5.15 GHz (Wi-Fi and Wi-Max).

#### 5. COMPARATIVE STUDY WITH LITERATURE

The proposed antenna has 4 elements with size of  $46 \times 46 \text{ mm}^2$  which is effectively very compact with respect to sited literature. It not only covers the N79 5G communication band but also exhibits commendable combined gain. Moreover, its diversity performance is notably strong. The proposed antenna with four elements gives better results than same size two element antennas.

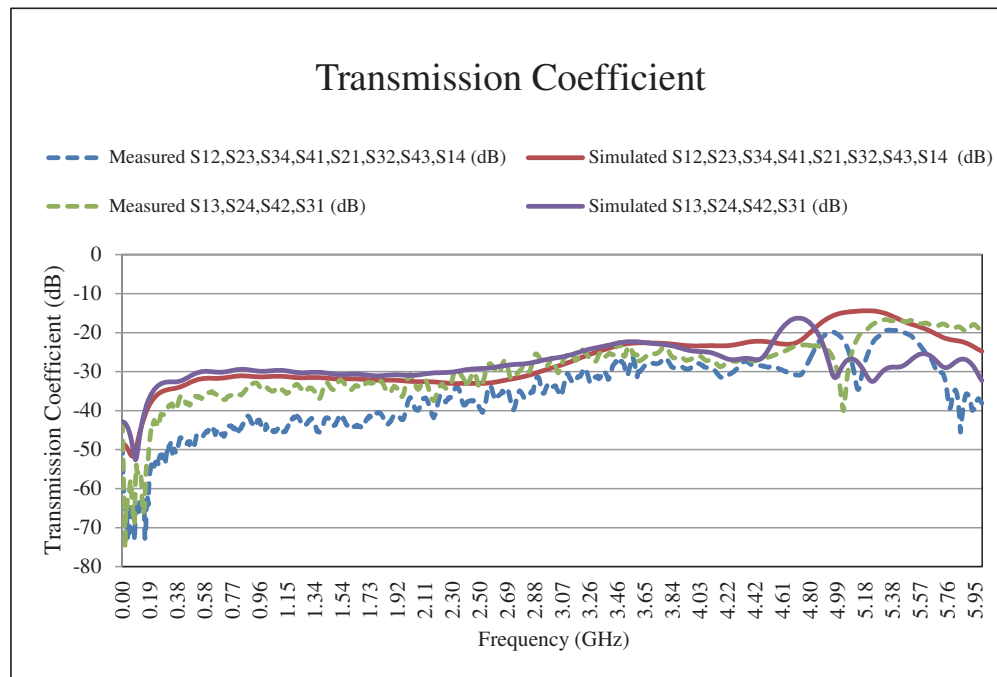


FIGURE 29. Comparison of transmission coefficients.

TABLE 1. Comparative analysis of proposed antenna.

Sr. No:	Referred antenna	Dimension ( $W \times L \times H$ ) mm <sup>3</sup>	No of Elements	Frequency Band	Maximum Gain	Efficiency	ECC	DG
1	Proposed design	$46 \times 46 \times 1.6$	4	4.72 GHz to 5.24 GHz	2.73 dB	> 60%	< 0.006	10
2	1	$46 \times 46 \times 1.6$	2	3.2 to 5.75 GHz	3.9 dB	81%	0.002	10
3	2	$6.8 \times 6.6 \times 4$	2	2.4 to 2.7 GHz 3.3 to 3.6 GHz	1.7 dB 2.13 dB	73%	< 0.21	-
4	3	$55 \times 35 \times 1.6$	2	2.74 to 12.33 GHz	2.9 dB		< 0.025	> 9.9
5	4	$62 \times 25.6 \times 1.524$	2	2.99 to 3.61 GHz	4.12 dB	> 72%	< 0.005	
6	5	$31.2 \times 31.2 \times 1.57$	2	24.25–27.5 GHz	4.732 dB	72.7%	0.03	15.8
7	6	$150 \times 75 \times 0.8$	4	3.4–3.6 GHz 4.8–5.0 GHz		50%	< 0.14 < 0.12	-
8	8	$11.4 \times 5.3 \times 0.8$	2	23 to 28 GHz	-	85%	< 0.001	> 9.8 dB

## 6. CONCLUSION

The antenna is designed with a monopole having twin matching stubs at the lower end with partial ground. The twin stubs are coupled with ground plane and produce capacitive effects. With the insertion of slot and variation in ground, the results are modified. The final design of patch antenna comprises twin stubs positioned at the lower end of the patch seamlessly integrated with E and C slots. The proposed MIMO antenna with four elements is suitable for 5G as well as other wireless applications. The four elements are identical to each other. They are placed

at equal distance from the center and orthogonal to each other. All the elements contain E and C shaped slots, and two identical stubs providing capacitive effect. The design shows the use of DGS which makes it more efficient. The antenna works over a band from 4.72 GHz to 5.24 GHz which covers 4.9 GHz WLAN, 5 GHz and 5.15 GHz Wi-Max and Wi-Fi bands. The gain of the intended antenna ranges from 2.23 dB to 2.73 dB for the desired bands. The scope for the future uses of the antenna spreads over a wide range of mobile applications and can also be used for Wi-Fi operations in medical fields as it provides better provisions.

## REFERENCES

- [1] Megahed, A. A., M. Abdelazim, E. H. Abdelhay, and H. Y. M. Soliman, "Sub-6 GHz highly isolated wideband MIMO antenna arrays," *IEEE Access*, Vol. 10, 19 875–19 889, 2022.
- [2] Jiang, W., Y. Cui, B. Liu, W. Hu, and Y. Xi, "A dual-band MIMO antenna with enhanced isolation for 5G smartphone applications," *IEEE Access*, Vol. 7, 112 554–112 563, 2019.
- [3] Biswas, A. K. and U. Chakraborty, "Compact wearable MIMO antenna with improved port isolation for ultra-wideband applications," *IET Microwaves Antennas & Propagation*, Vol. 13, No. 4, 498–504, Mar. 2019.
- [4] Sharma, P., R. N. Tiwari, P. Singh, P. Kumar, and B. K. Kanaujia, "MIMO antennas: design approaches, techniques and applications," *Sensors*, Vol. 22, No. 20, Oct. 2022.
- [5] Shoaib, N., S. Shoaib, R. Y. Khattak, I. Shoaib, X. Chen, and A. Perwaiz, "MIMO antennas for smart 5G devices," *IEEE Access*, Vol. 6, 77 014–77 021, 2018.
- [6] Ren, Z. and A. Zhao, "Dual-band MIMO antenna with compact self-decoupled antenna pairs for 5G mobile applications," *IEEE Access*, Vol. 7, 82 288–82 296, 2019.
- [7] Sangwan, M., G. Panda, and P. Yadav, "A literature survey on different MIMO patch antenna," in *Proceedings of The 5th International Conference on Inventive Computation Technologies (ICICT 2020)*, 912–918, Coimbatore, India, Feb. 2020.
- [8] Ahmad, A., D.-Y. Choi, and S. Ullah, "A compact two elements MIMO antenna for 5G communication," *Scientific Reports*, Vol. 12, No. 1, Mar. 2022.
- [9] Sharawi, M. S., "Printed multi-band MIMO antenna systems and their performance metrics," *IEEE Antennas and Propagation Magazine*, Vol. 55, No. 5, 218–232, Oct. 2013.
- [10] Bhunia, S. and P. P. Sarkar, "Reduced sized dual frequency microstrip antenna," *Indian Journal of Physics*, Vol. 83, No. 10, 1457–1461, Oct. 2009.
- [11] Guan, K., Z. Zhong, J. I. Alonso, and C. Briso-Rodriguez, "Measurement of distributed antenna systems at 2.4 GHz in a realistic subway tunnel environment," *IEEE Transactions on Vehicular Technology*, Vol. 61, No. 2, 834–837, Feb. 2012.
- [12] Li, M., X. Chen, A. Zhang, and A. A. Kishk, "Dual-polarized broadband base station antenna backed with dielectric cavity for 5G communications," *IEEE Antennas and Wireless Propagation Letters*, Vol. 18, No. 10, 2051–2055, Oct. 2019.
- [13] Das, S., P. P. Sarkar, and S. K. Chowdhury, "Investigations on miniaturized multifrequency microstrip patch antennas for wireless communication applications," *Journal of Electromagnetic Waves and Applications*, Vol. 27, No. 9, 1145–1162, 2013.
- [14] Rabbaa, A. and G. Dubost, "Analysis of a slot micro strip antenna," *IEEE Transactions on Antennas and Propagation*, Vol. 34, No. 2, 155–163, Feb. 1986.
- [15] Chakraborty, U., A. Kundu, S. K. Chowdhury, and A. K. Bhattacharjee, "Compact dual-band microstrip antenna for IEEE 802.11 a WLAN application," *IEEE Antennas and Wireless Propagation Letters*, Vol. 13, 407–410, 2014.
- [16] Liu, W.-C., C.-M. Wu, and Y. Dai, "Design of triple-frequency microstrip-fed monopole antenna using defected ground structure," *IEEE Transactions on Antennas and Propagation*, Vol. 59, No. 7, 2457–2463, Jul. 2011.
- [17] Prajapati, P. R., A. Patnaik, and M. V. Kartikeyan, "Improved DGS parameter extraction method for the polarization purity of circularly polarized microstrip antenna," *International Journal of RF and Microwave Computer-aided Engineering*, Vol. 26, No. 9, 773–783, Nov. 2016.
- [18] Prajapati, P. R. and S. B. Khant, "Gain enhancement of UWB antenna using partially reflective surface," *International Journal of Microwave and Wireless Technologies*, Vol. 10, No. 7, 835–842, Sep. 2018.